Comparison of exciplex generation under optical and X-ray excitation

A. A. Kipriyanov, A. R. Melnikov, D. V. Stass, and A. B. Doktorov

Comparison of exciplex generation under optical and X-ray excitation

A. A. Kipriyanov,[1] A. R. Melnikov,[1,2] D. V. Stass,[1,2] and A. B. Doktorov[1,2]
[1]V.V. Voevodsky Institute of Chemical Kinetics and Combustion, Novosibirsk, Russia
[2]Novosibirsk State University, Novosibirsk, Russia

Exciplex generation under optical and X-ray excitation in identical conditions is experimentally compared using a specially chosen model donor-acceptor system, anthracene (electron acceptor) and *N,N*-dimethylaniline (electron donor) in non-polar solution, and the results are analyzed and interpreted based on analytically calculated luminescence quantum yields. Calculations are performed on the basis of kinetic equations for multistage schemes of bulk exciplex production reaction under optical excitation and combination of bulk and geminate reactions of radical ion pairs under X-ray excitation. These results explain the earlier experimentally found difference in the ratio of the quantum yields of exciplexes and excited electron acceptors (exciplex generation efficiency) and the corresponding change in the exciplex generation efficiency under X-irradiation as compared to the reaction under optical excitation. *Published by AIP Publishing.* [http://dx.doi.org/10.1063/1.5001019]

I. INTRODUCTION

Luminescence methods are among the most sensitive experimental techniques and are widely used in various fields of physical chemistry. In such experiments, the required excited state can be obtained, e.g., by direct irradiation of solution of the molecule under study by the light of an appropriate wavelength producing photoluminescence. Ionizing X-irradiation of non-polar solutions is another method of generating excited states.[1,2] In this case, the key stage in the production of excited molecules is radical ion pair recombination proceeding by electron transfer from the radical anion to radical cation. In addition to radiation and internal radiationless deactivation, an electronically excited molecule in solution can also form a metastable bound state with another molecule. The formation of different excited complexes (exciplexes) in weakly polar and non-polar solvents has been actively studied since their discovery.[3] The interest is mostly focused on searching for new exciplex-forming systems and characterization of such complexes, as well as on exciplex application as a means of solving problems in adjacent fields. In particular, many studies are devoted to investigation of photo-induced electron transfer from an excited acceptor molecule to a donor that proceeds via intermediate exciplex generation.[4] At present, an important practical interest is connected with the possibility of using exciplex-forming systems as a convenient means of spectral adjustment of organic light-emitting diodes and increasing the efficiency of their electroluminescence.[5,6]

First, experimental studies of radiation-generated exciplexes were primarily confined to pyrene- or naphthalene-based systems (a standard case for optical excitation) in which the excited state lifetime is sufficient for the bulk reaction of excited complex generation to proceed.[7,8] When using such systems, specific features of excitation generation by ionizing radiation in which, as in electroluminescence,[9,10] the key stage of excited state generation is radical ion pair recombination were left unattended.

However, further experimental investigation of non-polar solutions of certain donor-acceptor systems revealed a difference in the spectra of their luminescence generated by optical and X-irradiation.[11] An increase in the quantum yield of the exciplex luminescence relative to the quantum yield of intrinsic luminescence of the excited molecule was detected experimentally under X-irradiation as compared to the case with optical excitation of the same sample. Furthermore, an efficient X-ray generation of optically inaccessible exciplexes for luminophores with very short intrinsic luminescence times was reported.[12] This indicates that in the given case the mechanism of exciplex formation substantially differs from the mechanism of exciplex production under optical excitation. It has been suggested[11] that the main distinction is a multistage character of exciplex generation due to competing geminate and bulk stages of recombination of the initially generated radical ion pairs under X-ray radiation.

To verify this assumption, in this work, we experimentally investigate the exciplex generation under optical and X-irradiation for a specially chosen model system, a mixture of anthracene and *N,N*-dimethylaniline (DMA) in non-polar solution. Here anthracene plays the role of the intrinsic luminophore, as well as the energy donor under optical excitation and electron acceptor under X-irradiation. DMA complements it by functioning as the energy acceptor under optical excitation and the electron donor under X-irradiation. We perform comparative experiments on the same samples in identical conditions, and theoretically calculate and compare exciplex generation efficiencies under optical and X-irradiation for varied mixture composition on the basis of two schemes.

Exciplex formation under optical excitation is described conventionally using a simple scheme that assumes optical excitation of the anthracene molecule that is subsequently deactivated by spontaneous radiation[13] or forms an exciplex with DMA, which emits in a different wavelength

range. Following Ref. 12, exciplex generation under X-irradiation is described on the basis of the simplest multistage scheme including both geminate and bulk reaction channels.

The performed analysis of the derived kinetic equations does show the change in exciplex formation efficiency under X-radiation in comparison with the reaction under optical excitation that follows from experimental data analysis and the corresponding change in the ratio between the calculated quantum yields of excited electron acceptor and exciplex.

II. EXPERIMENT

A. Materials and methods

All luminescence spectra given in this work were obtained using a homebuilt Magnetic–Field–Affected–Reaction–Yield (MARY) spectrometer with spectral resolution of fluorescence (grating monochromator MDR-206, LOMO, St. Petersburg, Russia, objective focus length 180 mm, grating 1200 lines mm^{-1}, inverse linear dispersion 4.3 nm mm^{-1}, and a FEU-100 PMT for detection) described in Ref. 14. The spectrometer allows one to obtain luminescence spectra under X-irradiation or optical excitation of the same samples in identical experimental conditions. Experimental spectra under X-irradiation were taken at the following settings: X-ray tube BSV-27 (Svetlana, St. Petersburg, Russia) 40 kV, 20 mA; detection channel monochromator slits 2.2 mm/2.2 mm (spectral resolution about 10 nm); PMT operating voltage 2200 V. X-radiation with the estimated dose rate of about 85 krad h^{-1} (at 40 kV/20 mA) produces a steady-state concentration of approximately 100 radical ion pairs uniformly distributed in the sample of the volume 1 ml. In the case of optical excitation, an XBO 150W/4 xenon lamp (OSRAM, Germany) with a double prism monochromator DMR-4 and a liquid light guide for excitation light transfer to the sample were used. The lamp operating current is 6.6 A, excitation wavelength is 345 nm, monochromator slits for the excitation channel are 1.5 mm/1.5 mm and for the detection channel are 2.2 mm/2.2 mm (spectral resolution about 10 nm), and PMT operating voltage is 2200 V.

All experimental spectra were recorded in identical cylindrical ampoules with an outer diameter 5 mm made from molybdenum glass which passes light with wavelength longer than 320 nm and produces almost no intrinsic luminescence under X-ray radiation, in stark contrast to quartz. The samples containing 0.3 ml of solution were degassed by repeated freeze-pump-thaw cycles and sealed off in their ampoules. To further suppress intrinsic radiation-generated luminescence of the glass, the ampoules were placed in a lead jacket with openings for the excitation beam and detected luminescence. In the case of optical excitation, the samples were also put in the same jacket to keep conditions identical. A detailed description of the choice of ampoule material and experiment geometry is given in Ref. 14. All luminescence spectra presented in this work contain 256 wavelength points and are averaged over 16 independent wavelength scans for X-irradiation or 4 scans for optical excitation. The luminescence intensity is

given in relative units corresponding to the PMT output signal. Correction for spectral sensitivity curves was not applied, as in the employed wavelength range the correction curve is essentially flat. Correction for baseline was performed by averaging over a long wavelength tail of the spectrum containing no luminescence and subtracting the obtained average from the entire spectrum. All spectra were recorded at room temperature.

Luminescence spectra under X-irradiation and optical excitation were obtained for the same set of seven samples with the concentration of DMA varying in the range from $1 \cdot 10^{-3}$ M to $9 \cdot 10^{-2}$ M and the anthracene concentration was equal to $2 \cdot 10^{-4}$ M in all the samples. The optical density of the sample solution at the excitation wavelength is determined only by anthracene absorption and is equal to 0.15 ($\varepsilon_{345} \approx 2900$ M^{-1} cm^{-1}), and DMA shows almost no absorption at this wavelength.[15] First, luminescence spectra of all seven samples were obtained under optical excitation at 345 nm, and then the entire set was measured under X-irradiation.

As a solvent, additionally purified isooctane (2,2,4-trimethylpentane) was used which is a typical non-luminescent alkane with a quantum yield less than 10^{-5} and an excited state lifetime shorter than 0.2 ns.[16,17] An alkane is generally essential to produce recombining radical ion pairs under X-irradiation.[1,2] Isooctane further makes it possible to exclude the channel of radiationless energy transfer from excited solvent molecules to solutes (DMA or anthracene).[18] Thus, under X-irradiation of isooctane solutions, electronically excited states of donor or acceptor are generated solely as a result of radical ion pair recombination which significantly simplifies the reaction scheme. On the other hand, under optical excitation, there is no crucial difference between isooctane and any other linear or branched alkane. DMA was freshly distilled over zinc powder, fraction with bp 193–195 °C was used. Anthracene (99%, Aldrich) was used without additional purification.

B. Results

Figure 1 shows a selection of luminescence spectra recorded at identical experimental conditions under optical excitation at 345 nm and under X-irradiation, respectively, for samples with DMA concentration in the mixture varying from $1 \cdot 10^{-3}$ M to $9 \cdot 10^{-2}$ M. In both cases, the luminescence spectra of mixtures comprise intrinsic anthracene luminescence in the form of a resolved structure in the region of 25 000 cm^{-1} (400 nm), the intensity of which decreases with increasing DMA concentration in the mixture. Spectra also show a long wavelength structureless emission band of exciplex ($\sim$21 000 cm^{-1}, 480 nm), the intensity of which increases with increasing DMA concentration. Under X-irradiation, the luminescence spectra of the mixtures also have a prominent intrinsic DMA luminescence ($\sim$29 000 cm^{-1}, 350 nm), the intensity of which increases with increasing DMA concentration in the mixture. Note also the different x-axis scale for the two panels: spectra under optical excitation were taken only up to 28 000 cm^{-1}, i.e., down to the edge of the excitation line at 345 nm.

Following Ref. 11, all experimental luminescence spectra were decomposed into sums of spectra of individual
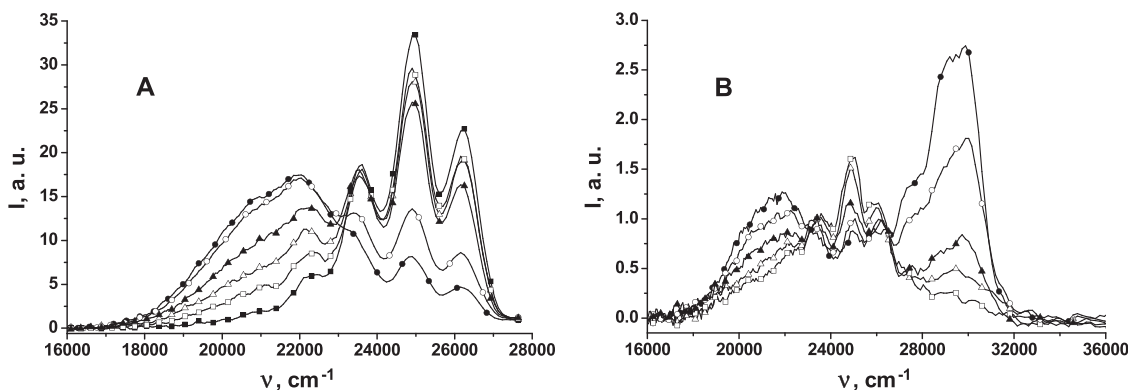
FIG. 1. (a) Averaged luminescence spectra of anthracene/DMA mixtures in isooctane under optical excitation at 345 nm. Anthracene concentration in the mixture $2 \cdot 10^{-4}$ M for all samples; concentration of DMA: ●—$6 \cdot 10^{-2}$ M; ○—$3 \cdot 10^{-2}$ M; ▲—$1 \cdot 10^{-2}$ M; △—$7 \cdot 10^{-3}$ M; □—$4 \cdot 10^{-3}$ M; ■—$1 \cdot 10^{-3}$ M. (b) Averaged luminescence spectra of anthracene/DMA mixtures in isooctane under X-irradiation. Anthracene concentration in the mixture $2 \cdot 10^{-4}$ M for all samples; concentration of DMA: ●—$6 \cdot 10^{-2}$ M; ○—$3 \cdot 10^{-2}$ M; ▲—$1 \cdot 10^{-2}$ M; △—$4 \cdot 10^{-3}$ M; □—$1 \cdot 10^{-3}$ M.

emission components. Under optical excitation, the luminescence spectra were the contributions from anthracene and exciplex, while under X-irradiation, emissions from anthracene, DMA, and exciplex were resolved. Each component was represented by a set of Gaussian functions using the *FindFit* function in Wolfram Mathematica 7 environment. Decomposition was performed in wavenumbers, and the overall shapes of the component spectra were considered fixed. The only varied parameters were the contributions from each emission component to the total luminescence spectrum, i.e., two or three relative weights for optical excitation and X-irradiation, respectively. When converting the experimental luminescence spectra from wavelengths to wavenumbers, the spectra were not multiplied by λ^2 [19] to avoid reduction in the signal-to-noise ratio which was especially critical for experiments under X-irradiation. This is possible, since we employ the ratio of emission intensities for exciplex and anthracene $K = I_{ex}/I_{antr}$ (see Fig. 5 below) as a measure of exciplex generation efficiency under optical excitation and X-irradiation. It was verified that the desired ratio of ratios K_{X-ray} and K_{Light} did not depend on specific spectrum representation, since the same shapes of luminescence bands for anthracene, exciplex, and DMA were used for decomposition of experimental spectra taken both under optical excitation and under X-irradiation. Decompositions of experimental spectra with intensity scaling by λ^2, as well as in the more advanced and correct transition dipole moment representation,[20] are given in the supplementary material to this paper. For the purpose of this work, all methods of decomposition produced essentially the same result.

Luminescence band shapes of the individual emission components were obtained separately in independent experiments. To correctly describe the intrinsic luminescence band shapes for anthracene and DMA, we used the luminescence spectrum for the solution of $2 \cdot 10^{-4}$ M anthracene in isooctane under optical excitation at 345 nm and the luminescence spectrum for the solution of 10^{-2} M DMA in isooctane under X-irradiation, respectively. These spectra were obtained independently in the same experimental conditions as the spectra for mixtures and were subsequently represented as a minimum set of Gaussian functions (5 for anthracene and 3 for DMA)

using the same fitting approach. After fitting, the position, width, and relative peak amplitude for each Gaussian function were fixed. This gave an analytical approximation for noisy experimental spectra which made the procedure of full spectral decomposition described above more robust and reduced the number of independent fitting parameters per emission component to just the overall amplitude of the composite line shape. The results of the Gaussian representation of the intrinsic luminescence spectra for anthracene and DMA are given in Fig. SI1 of the supplementary material.

The shape of the exciplex emission band in the system anthracene–DMA was obtained by the procedure described in Ref. 21 based on the significant difference in the degree of quenching of intrinsic luminescence of the relatively short-lived excited state of anthracene ($\tau_f = 5.6$ ns[22]) and long-lived exciplex ($\tau_f \sim 70 \pm 3$ ns[21]) by dissolved oxygen. Exciplex emission band was obtained by subtracting from the luminescence spectrum of a degassed mixture of anthracene and DMA the spectrum of the same mixture equilibrated with atmosphere. Original experimental spectra of radiation-induced luminescence from degassed samples and samples at atmospheric pressure for the system anthracene–DMA were given in Ref. 21. The exciplex emission band shape thus obtained and its representation as the minimum set (two) of Gaussian functions with fixed position, width, and relative peak amplitude are shown in Fig. 2.

Using the luminescence band shapes of anthracene, DMA, and exciplex described above as a fixed input, all experimental luminescence spectra of anthracene/DMA mixtures obtained under optical excitation or X-irradiation were decomposed into the sums of spectra of the individual emission components (anthracene, exciplex under optical excitation; anthracene, DMA, exciplex under X-irradiation). Typical examples of the experimental spectra of anthracene/DMA mixtures under optical excitation and X-irradiation and their decomposition are given in Fig. 3.

Further, we plotted the ratio I_{ex}/I_{antr} vs. DMA concentration in the mixture for optical excitation and X-irradiation, where the relative luminescence intensities I_{antr} and I_{ex} were determined from the decomposed spectra as the area under the luminescence band of anthracene and exciplex, respectively.
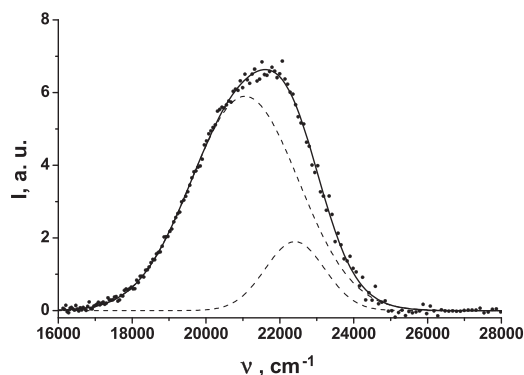
FIG. 2. Decomposition of the exciplex emission spectrum in the system anthracene/DMA into two Gaussian functions is shown by dashed lines. Points indicate the experimental spectrum obtained by the procedure described in Ref. 21. In the subsequent decomposition of spectra from mixtures, the spectrum shape of exciplex emission was described by the fixed sum of Gaussian functions shown by a solid line.

Integration was performed on the corresponding analytical sum of Gaussian functions in the range from 15 000 cm^{-1} to 27 000 cm^{-1} for the anthracene luminescence band and from 17 000 cm^{-1} to 29 000 cm^{-1} for the exciplex luminescence band. The dependences thus obtained are given in Fig. 4. In such coordinates each experimental spectrum, i.e., each composition of the mixture, is represented by one point. All in all,

luminescence spectra for seven mixtures with different concentrations of DMA, as well as for anthracene solution with concentration $2 \cdot 10^{-4}$ M in isooctane corresponding to zero DMA concentration, were obtained and processed.

Using the dependences given in Fig. 4, one can compare the exciplex generation efficiency under optical excitation and X-irradiation referred to the number of excited states of anthracene in solution. For this purpose, the dependence of the ratio $\xi = \frac{K_{X\text{-ray}}}{K_{Light}}$ on DMA concentration in the mixture was derived, where $K_{X\text{-ray}}$ and K_{Light} are the ratios I_{ex}/I_{antr} (Fig. 4) for X-irradiation and optical excitation, respectively. The obtained dependence in the studied range of DMA concentrations is shown in Fig. 5.

It is seen from Fig. 5 that at DMA concentrations in the mixture less than 0.03 M, exciplexes are generated more efficiently under X-irradiation than under optical excitation, which may be qualitatively explained by the presence of additional channels of exciplex formation. At higher DMA concentrations, exciplex generation efficiency in the given system (anthracene/DMA) for X-irradiation and optical excitation is almost the same. Earlier, a similar effect of a more efficient exciplex generation for the case of X-irradiation was observed for mixtures naphthalene/DMA[12] and anthracene/DMA[11] in *n*-dodecane at varied concentration of naphthalene or anthracene, respectively. In these papers,
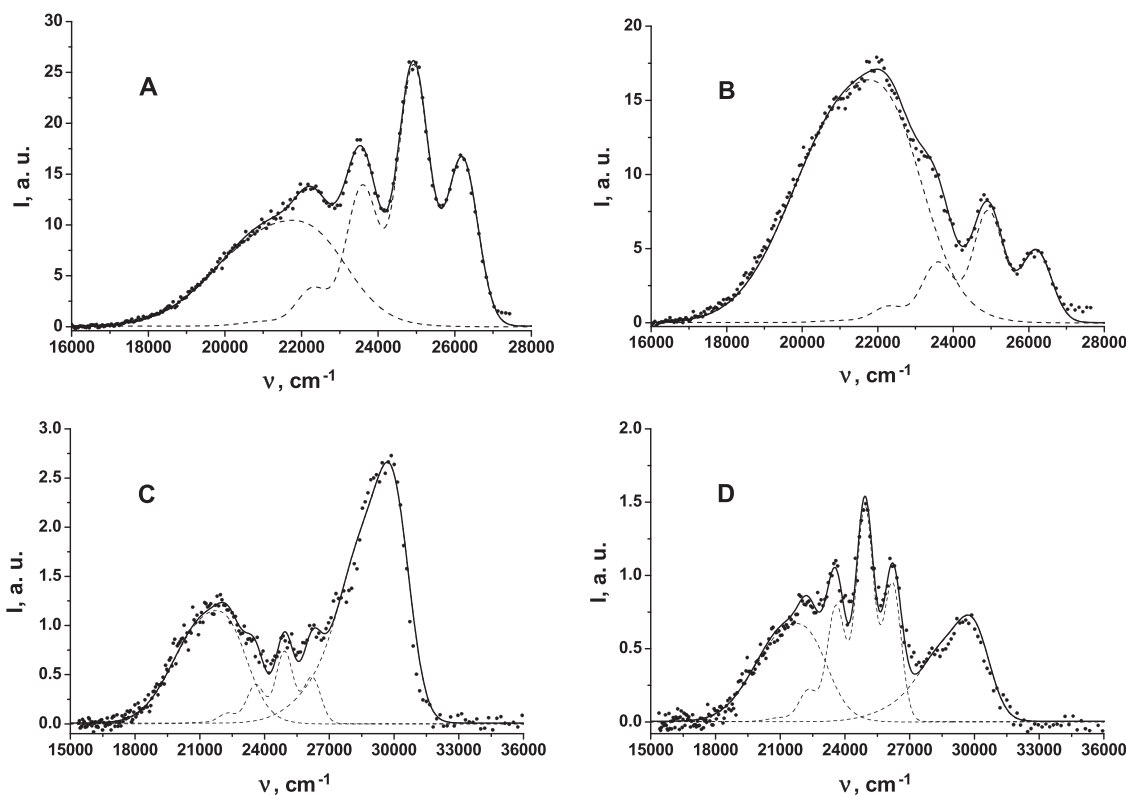

FIG. 3. Decomposition of the luminescence spectra taken under optical excitation at 345 nm [(a) and (b)] or X-irradiation [(c) and (d)] for anthracene/DMA mixtures at concentrations (a) $2 \cdot 10^{-4}$ M and $1 \cdot 10^{-2}$ M; (b) $2 \cdot 10^{-4}$ M and $6 \cdot 10^{-2}$ M; (c) $2 \cdot 10^{-4}$ M and $6 \cdot 10^{-2}$ M; (d) $2 \cdot 10^{-4}$ M and $7 \cdot 10^{-3}$ M, respectively, in isooctane (points) into two [right to left: anthracene, exciplex, spectra (a) and (b)] or three [right to left: DMA, anthracene, exciplex, spectra (c) and (d)] constituent emission components indicated by dashed lines. The obtained reconstruction of the spectrum shape of the mixture as the sum of two or three components for optical excitation or X-irradiation, respectively, is shown by a solid line. Only two numerical parameters, the amplitudes of the emission bands for exciplex and anthracene, were varied under optical excitation, and three parameters, the amplitudes of the emission bands for exciplex, anthracene, and DMA, were varied under X-irradiation.
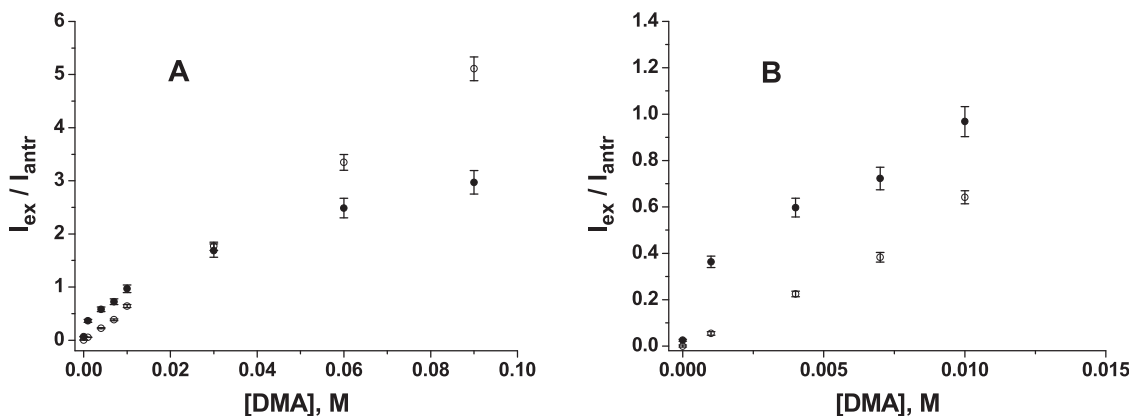
FIG. 4. Experimental dependences of the ratio I_{ex}/I_{antr} on DMA concentration in the mixture (see text for details), (a) ∘—optical excitation at 345 nm; •—X-irradiation; (b) subplot of **A** in the range of low DMA concentrations. Error bars are 95% confidence intervals for each experimental point.

the more efficient generation of exciplexes under X-irradiation was qualitatively attributed to the additional possibility of exciplex generation via recombination of secondary radical ion pairs. Secondary radical ion pairs, for example, consisting of radical cations of DMA and radical anions of anthracene for the system anthracene/DMA are formed via charge capture from primary radical ion pairs (solvent radical cation and electron) resulting from ionization of a solvent molecule by X-radiation.[23] Since at the moment of recombination the pair partners are close to each other, at the distance of 10–15 Å, after recombination the excited molecule and its partner are also close together, so additional efficient generation of exciplex becomes possible. The scheme of exciplex generation under X-irradiation proposed in the cited papers qualitatively accounted for the observed fact of a more efficient production of excited complexes; however, theoretical treatment of this scheme is absent. The exciplex generation is expected to occur via recombination of secondary radical ion pairs, and this additional channel is taken into account in the theoretical treatment of exciplex generation under X-irradiation on the basis of the multistage scheme. Furthermore, in photochemistry, it is common practice to study the exciplex generation efficiency as a function of the quencher concentration the role

of which in the given case is played by DMA. Variation of the concentration of the excited component for its low optical densities at excitation wavelength should produce a qualitatively clear dependence under optical excitation. An increase in the concentration of the excited component leads to a proportional enhancement of exciplex generation via the bulk channel. The dependence of the exciplex generation efficiency on the excited component concentration is not trivial under X-irradiation due to the multistage character of exciplex generation and competition of bulk and geminate reaction channels. For this reason, the experiment described in this paper was deliberately conducted in conditions natural for photochemistry and on a system simultaneously convenient for both photo- and radiation-chemistry. Section III presents the theory developed for its interpretation.

III. THEORY

To interpret the observed increase in the exciplex generation efficiency under X-irradiation as compared to optical excitation, in this section, we consider the corresponding simplest possible schemes of multistage reactions of exciplex generation for the two types of irradiation. To make direct comparison possible, schemes for optical excitation and X-irradiation are formulated in common terms and using the same notations. For these schemes, kinetic equations are given that are the basis for theoretical calculation of the corresponding quantum yields of luminescence. Kinetic equations of the multistage reaction (containing geminate and bulk channels) of exciplex generation under X-irradiation (that can be obtained by consistent derivation) are written and physically interpreted. The derivation itself and the detailed theoretical treatment of the behavior of the target quantities with varying concentrations of electron donor (excited molecule quencher) will be the subject of a separate publication.

FIG. 5. Experimental dependence of the ratio $K_{\text{X-ray}}/K_{\text{Light}}$ of exciplex generation efficiency under X-irradiation and optical excitation on DMA concentration in the mixture (see text for details). Error bars are 95% confidence intervals calculated by the error propagation law.

A. Exciplex generation under optical excitation

The reaction of exciplex $E = [AD]^*$ formation due to the irreversible bulk reaction of an optically excited molecule A^* of electron acceptor (energy donor) A with electron donor (quencher) D is described on the basis of a simple scheme
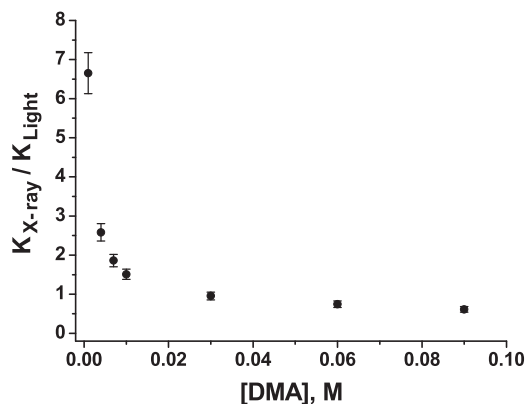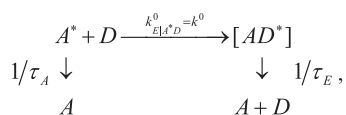
that assumes the decay of excited molecule A^* via two channels, i.e., deactivation by radiation and radiationless decay, as in conventional consideration of luminescence quenching,[13] and by exciplex production. The formed exciplexes are also deactivated by radiation and radiationless decay

$$A^* + D \xrightarrow{k^0_{E|A^*D}=k^0} [AD^*]$$
$$1/\tau_A \downarrow \qquad\qquad \downarrow 1/\tau_E ,$$
$$A \qquad\qquad A + D$$

SCHEME 1. Exciplex generation under optical excitation.

where $\tau_A = 1/\left(k^F_A + k_A\right)$ and $\tau_E = 1/\left(k^F_E + k_E\right)$ are the lifetimes of the acceptor and exciplex excited state, respectively, k^F_A and k^F_E are the rate constants of the acceptor and exciplex decay by spontaneous light emission, k_A and k_E are the rate constants of radiationless decay. Note that, in principle, radiationless exciplex decay may involve the bulk reaction of exciplex dissociation into a charge pair, i.e., $E \rightarrow A^{-\bullet} + D^{+\bullet}$.[24–28] As is common for non-polar solvents (Weller scheme I[24,25]), in this scheme, we assume the absence of bulk reaction of irreversible charge transfer

$$A^* + D \rightarrow A^{-\bullet} + D^{+\bullet} \qquad (3.1)$$

with subsequent exciplex generation.

Furthermore, in our case of a non-polar solvent, the reaction of exciplex generation (according to Scheme 1) is considered irreversible.[29] The rate of exciplex formation is determined by the rate of the elementary event $w(q) \equiv w_{E|A^*D}(q)$ of the $A^* + D$ pair association into product E. In the general case, this rate depends on the coordinate q in the configuration space of the reacting pair (including both relative-position vector $\vec{r}$ and Euler angles of molecular axes orientation of reactants relative to the laboratory reference system, and other classical internal degrees of freedom, for example, orientation of internal molecular groups of reactants). Depending on the employed reaction model, in the following, we shall use the specific representation of the configuration space (for instance, only the relative-position vector $\vec{r}$ or the distance r between reactants).

The quantity $k^0_{E|A^*D} = k^0$ appearing in kinetic Scheme 1 is the reaction rate constant of the bulk irreversible reaction which in the general case is related to the elementary event rate as

$$k^0 = k^0_{E|A^*D} = \int w_{E|A^*D}(q)\varphi(q)\,dq = \int w(q)\varphi(q)\,dq, \qquad (3.2)$$

where $\varphi(q)$ is the equilibrium distribution in the configuration space coordinates (the Gibbs distribution in the thermodynamic limit).

Further, we examine the standard case where electron donor D is in excess with respect to excited acceptor A^*, i.e., $[A^*]_t \ll [D]_t \equiv [D] = Const.$; this corresponds to consideration of pseudo-monomolecular reaction and experimental conditions. In this situation, in the framework of a commonly used approach (relying on the Waite-Smoluchowski type equations[30–33]), equations for the concentrations $[A^*]_t$ and $[E]_t$ of

the excited molecules and exciplexes, respectively, have the form

$$\frac{d}{dt}[A^*]_t = -\frac{1}{\tau_A}[A^*]_t - K(t)[A^*]_t[D],$$
$$\frac{d}{dt}[E]_t = -\frac{1}{\tau_E}[E]_t + K(t)[A^*]_t[D], \qquad (3.3)$$

with the initial conditions $[A^*]_{t=0} = [A^*]_0$ and $[E]_0 = 0$. The first equation in (3.3) is traditional for the description of luminescence quenching,[13] while the second one describes the accumulation and decay of exciplexes. The time-dependent reaction rate constant $K(t)$ is determined by diffusion and reaction dynamics, and its form depends on the particular model of the reacting system. The most widely known models include diffusion-controlled contact reaction of rigid spheres,[31] more general diffusion-influenced contact reaction of rigid spheres,[32] or remote diffusion-influenced reactions.[33–35] More complicated models that allow for reactivity anisotropy are also available in the literature.[36] With time, the above rate constant (after the end of the so-called transient stage) attains its steady-state value (sometimes called the Markovian rate constant[33])

$$\lim_{t\to\infty} K(t) = k, \qquad (3.4)$$

and kinetic equations (3.3) (neglecting the transient stage) correspond to the kinetic equations of formal chemical kinetics (Markovian kinetic equations[33]) based on the kinetic law of mass action.

Differential equations (3.3) are convenient for calculating the kinetics of the process under study. However, they are not convenient for the calculation of the quantum yields of excited molecules and exciplexes we are interested in. Therefore, restricting ourselves to the consideration of dilute solutions, we describe the reactions for which the so-called binary approximation is valid (taking into account only pair encounters of reactants in solution) using the integro-differential equations of the Modified Encounter Theory (MET) equivalent to Eq. (3.3),[33,37–39]

$$\frac{d}{dt}[A^*]_t = -\frac{1}{\tau_A}[A^*]_t - [D]\int_{-0}^{t}\kappa(t-\tau)[A^*]_\tau\,d\tau,$$
$$\frac{d}{dt}[E]_t = -\frac{1}{\tau_E}[E]_t + [D]\int_{-0}^{t}\kappa(t-\tau)[A^*]_\tau\,d\tau, \qquad (3.5)$$

where the Laplace transform (denoted by superscript L, s is the Laplace variable) of the kernel of kinetic equations (3.5) can be expressed[39] in terms of the Laplace transform of the rate constant

$$\kappa^L(s) = \Sigma^L\left(s + \frac{1}{\tau_A} + k[D]\right), \qquad (3.6)$$

where $\Sigma^L(s) = sK^L(s)$ is the Laplace transform of the Integral Encounter Theory (IET) kernel expressed in terms of the Laplace transform of the rate constant[39] and $k = \lim_{s\to 0} sK^L(s) = \Sigma^L(0)$ is the steady-state constant defined in Eq. (3.4). Note that, neglecting the transient stage, we have

$$K^L(s) \approx \frac{k}{s} \quad \text{or} \quad \Sigma^L(s) \approx k. \qquad (3.7)$$

In view of Eq. (3.6), Eq. (3.5) readily gives the Laplace transforms of the concentrations of the excited molecules and exciplexes from which the desired quantum yields are easily obtained,

$$
\eta_{A^*} = k_A^F \frac{[A^*]^L (s=0)}{[A^*]_0} = \frac{k_A^F}{\frac{1}{\tau_A} + [D] \Sigma^L \left(\frac{1}{\tau_A} + k[D] \right)},
$$

$$
\eta_E = k_E^F \frac{[E]^L (s=0)}{[A^*]_0} = \frac{\tau_E k_E^F [D] \Sigma^L \left(\frac{1}{\tau_A} + k[D] \right)}{\frac{1}{\tau_A} + [D] \Sigma^L \left(\frac{1}{\tau_A} + k[D] \right)}. \tag{3.8}
$$

The dependence of the ratio of the quantum yields of the excited molecule in the absence and in the presence of the quencher D (electron donor) on its concentration $[D]$ has the form

$$
\frac{\eta_{A^*}([D]=0)}{\eta_{A^*}} = 1 + \tau_A [D] \Sigma^L \left(\frac{1}{\tau_A} + k[D] \right) \equiv 1 + \tau_A [D] k_q, \tag{3.9}
$$

where the quenching rate constant is introduced[13,39]

$$
k_q = \Sigma^L \left(\frac{1}{\tau_A} + k[D] \right) = \left(\frac{1}{\tau_A} + k[D] \right) K^L \left(\frac{1}{\tau_A} + k[D] \right). \tag{3.10}
$$

Without regard to the transient stage [see. Eq. (3.7)], the quenching rate constant does not depend on the concentration $[D]$ and coincides with the steady-state reaction rate constant k, while dependence (3.9) is linear and obeys the Stern-Volmer law.[13] With the transient stage taken into account, in the general case, there exist deviations from linear dependence. However, if $k[D] \ll \frac{1}{\tau_A}$, then the Stern-Volmer law is fulfilled, but the quenching rate constant does not coincide with the steady-state reaction rate constant k and is as follows:

$$
k_q \approx \Sigma^L \left(\frac{1}{\tau_A} \right) = \frac{1}{\tau_A} K^L \left(\frac{1}{\tau_A} \right). \tag{3.11}
$$

The sought ratio of the quantum yields of exciplexes η_E and excited molecules η_{A^*} in the case of optical initiation of the process is

$$
K_{\text{Light}} = \frac{\eta_E}{\eta_{A^*}} = \frac{k_E^F}{k_A^F} \tau_E [D] \Sigma^L \left(\frac{1}{\tau_A} + k[D] \right) \equiv \frac{k_E^F}{k_A^F} \tau_E [D] k_q \tag{3.12}
$$

and, within the limits of validity of the Stern-Volmer law, is a linear function of concentration $[D]$ of the electron donor (excitation quencher).
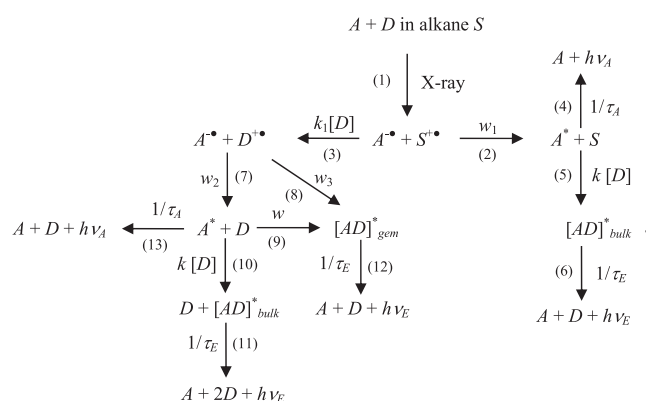
B. Exciplex generation under X-irradiation

To describe the reaction of exciplex generation under X-irradiation, a multistage scheme was constructed that included both geminate and bulk channels (Scheme 2).

We shall formally describe the process presented in Scheme 2 as a multistage geminate reaction of diffusing isolated pairs of reacting radicals (although bulk stages of exciplex formation are also present). Let us take that at the initial moment of time X-irradiation produces geminate pair

$A^{-\bullet} + S^{+\bullet}$ which subsequently transforms to other geminate pairs and bound states. We omit the details of the primary pair production considering this state as prescribed at the initial moment of time.

Geminate stages of the process are taken into account by introducing the corresponding probabilities of elementary events. Electron acceptor luminescence quenching in the geminate pair and generation of the exciplex $A^* + D \xrightarrow{w} E_{gem} = [A\,D]^*_{gem}$ (stage 9) is defined by the rate $w(q)$ of the elementary event. Electron transfer in the radical ion pair to the solvent molecule $A^{-\bullet} + S^{+\bullet} \xrightarrow{w_1} A^* + S$ (stage 2) is defined by the rate $w_1(q)$. Electron transfer to the electron acceptor $A^{-\bullet} + D^{+\bullet} \xrightarrow{w_2} A^* + D$ (stage 7) is defined by the rate $w_2(q)$. Radical ion pair recombination $A^{-\bullet} + D^{+\bullet} \xrightarrow{w_3} E_{gem} = [A\,D]^*_{gem}$ (stage 8) is defined by the rate $w_3(q)$,

SCHEME 2. Multistage reaction proceeding after X-irradiation of the system $A + D$ in alkane S.

Bulk reactions (bulk channel of exciplex formation $A^* + D \xrightarrow{k^0} E_{bulk} = [A\,D]^*_{bulk}$ (stages 5 and 10) coinciding with the bulk channel under optical excitation described in Sec. III A) and electron transfer from donor to solvent $S^{+\bullet} + D \xrightarrow{k_1^0} S + D^{+\bullet}$ (stage 3) in the framework of the "geminate" approach are taken into consideration as stages of monomolecular transformations in the corresponding geminate pairs that proceed with rates $k[D]$ and $k_1[D]$, respectively. This corresponds to the widely known "scavenger problem," see Refs. 40 and 41 and the references therein. Reaction rate constants k and k_1 are steady-state rate constants defined by recipe (3.4) for the corresponding bulk channel. In such a treatment, transient stages of the bulk reactions in question are ignored. An approximate account of such stages in calculating quantum yields may be taken by replacing the steady-state rate constants by the corresponding quenching rate constants by recipe (3.11).

For non-polar solutions, all elementary stages of the multistage reaction under study may be considered irreversible. Luminescence of the exciplexes and excited electron acceptors, as well as radiationless deactivation, are taken into account by introducing intrinsic lifetimes τ_E and τ_A (stages 4, 6, 11, 12, 13).

The description of the multistage process as it is formulated above calls for the use of kinetic approach in the theory of

geminate reactions. The kinetic approach is different from the conventional one which is based on the calculation of survival probabilities in geminate pairs. The kinetic approach makes it possible to derive kinetic equations for the mean concentrations of reactants in the thermodynamic limit or probabilities of finding them in the reacting system. It thus allows one to consider reactants formed in geminate pairs and bulk reactions on equal terms. Furthermore, in the framework of the kinetic approach to geminate reactions, just as in the theory of multistage bulk reactions, consideration using the matrix formalism relying on the concept of "effective particles"[42] is possible. General matrix kinetic theory of multistage geminate reactions has been developed in Ref. [42], where the limits of the applicability of the proposed method are indicated, and the physical meaning of kinetic equations is explained. In the present contribution, this theory is applied to the examination of concrete kinetic Scheme [2] of the multistage reaction course. This calls for the calculation of the corresponding matrix elements in the general theory.[42] The detailed calculation of such elements aimed at obtaining kinetic equations for a specific multistage reaction under study is rather cumbersome and will be presented in a future dedicated paper. In this work, we shall use the derived kinetic equations and give clear physical interpretation of them.

The kinetics of acceptors A^* is defined by the probability $p_{A^*}(t)$ of finding this acceptor in the reaction system at the moment of time t. The corresponding exciplex kinetics $p_E(t)$ is defined by the sum of contributions from bulk and geminate channels $p_E(t) = p_{E_{bulk}}(t) + p_{E_{gem}}(t)$. For the Laplace transforms of the sought probabilities $p_{A^*}(t)$ and $p_{E_{bulk}}(t)$ of finding excited molecules of acceptors and exciplexes arisen from bulk reactions in the reacting system, respectively, and the probability $p_{E_{gem}}(t)$ of finding the exciplexes formed as a result of geminate association in the reacting system, we have

$$\begin{cases} sp_{A^*}^L(s) = -\left(k\,[D] + \dfrac{1}{\tau_A}\right) p_{A^*}^L(s) + I_A^L(s), \\[2mm] sp_{E_{bulk}}^L(s) = -\dfrac{1}{\tau_E} p_{E_{bulk}}^L(s) + k\,[D]\, p_{A^*}^L(s), \\[2mm] sp_{E_{gem}}^L(s) = -\dfrac{1}{\tau_E} p_{E_{gem}}^L(s) + I_E^L(s). \end{cases} \quad (3.13)$$

Equations (3.13) have a clear physical meaning when considered in the time domain (see Scheme [2]). Time variation of the probability to find reactant A^* is determined by its monomolecular decay at the rate $\frac{1}{\tau_A}$ (stages 4 and 13) and the decay due to the bulk reaction of exciplex generation (stages 5 and 10) at the rate $k[D]$, as well as by its accumulation described by the inhomogeneous term (source) $I_A(t)$ defined by the corresponding geminate reactions. The time evolution of the probability of finding exciplex E_{bulk} is determined by its monomolecular decay (stages 6 and 11) at the rate $\frac{1}{\tau_E}$ and its generation from reactant A^* at the rate $k[D]$ due to bulk reactions (stages 5 and 10). Time variation of the probability of finding exciplex E_{gem} is determined by its monomolecular decay at the rate $\frac{1}{\tau_E}$ (stage 12) and its accumulation described by the inhomogeneous term (source) $I_E(t)$ defined by the corresponding geminate reactions.

The source term $I_A(t)$ defines the formation of reactant A^* from geminate pairs $A^{-\bullet} + S^{+\bullet}$ (stage 2) and $A^{-\bullet} + D^{+\bullet}$ (stage 7) at the rates $w_1(q)$ and $w_2(q)$, respectively, and its decay in geminate pair $A^* + D$ (containing A^*) as a result of exciplex E_{gem} generation (stage 9) at the rate $w(q)$. The source $I_E(t)$ defines exciplex E_{gem} formation as a result of geminate reactions in pairs $A^{-\bullet} + D^{+\bullet}$ (stage 8) and $A^* + D$ (stage 9) at the rates $w_3(q)$ and $w(q)$, respectively. In agreement with the above reasoning, the Laplace transforms of the inhomogeneous terms (sources) appearing in Eq. (3.13) have the form

$$\begin{aligned} I_A^L(s) &= \iint dq\,dq' \left[\left(w_1(q)\, g_1^L(q|q';s) + w_2(q)\, g_2^L(q|q';s) - w(q)\, g_3^L(q|q';s) \right) f(q') \right], \\ I_E^L(s) &= \iint dq\,dq' \left[\left(w_3(q)\, g_2^L(q|q';s) + w(q)\, g_3^L(q|q';s) \right) f(q') \right]. \end{aligned} \quad (3.14)$$

Here $f(q)$ is the initial distribution (in the configuration space q) in geminate pair $A^{-\bullet} + S^{+\bullet}$ generated by X-irradiation, while $g_1^L(q|q';s)$, $g_2^L(q|q';s)$, and $g_3^L(q|q';s)$ are the Laplace transforms of the propagator kernels that describe the evolution in pairs $A^{-\bullet} + S^{+\bullet}$, $A^{-\bullet} + D^{+\bullet}$, and $A^* + D$, respectively. It is assumed that upon transformation of geminate pairs due to chemical conversions the configuration space coordinate q remains unchanged. The closed set of equations for the resolvent kernels has the form

$$\begin{cases} \left(s - \hat{L}_1(q) + k_1[D] + w_1(q)\right) g_1^L(q|q';s) = \delta(q - q'), \\[2mm] \left(s - \hat{L}_2(q) + w_2(q) + w_3(q)\right) g_2^L(q|q';s) = k_1[D] g_1^L(q|q';s), \\[2mm] \left(s - \hat{L}_3(q) + \left(k_q[D] + \dfrac{1}{\tau_A}\right) + w(q)\right) g_3^L(q|q';s) = w_2(q) g_2^L(q|q';s) \end{cases} \quad (3.15)$$

and also allows a clear physical interpretation in the time domain. The propagator $g_1(q|q';t)$ which is the conditional probability density of finding geminate pair $A^{-\bullet} + S^{+\bullet}$ at the instant of time t with coordinate q if at the initial instant of time this coordinate was q' changes as a result of the

relative diffusion motion of reactants of this pair [defined by a functional operator $\hat{L}_1(q)$], as well as due to bulk reaction (stage 3) of the pair $A^{-\bullet} + D^{+\bullet}$ generation at the rate $k_1[D]$ and geminate reaction (stage 2) of the pair $A^* + S$ generation at the rate $w_1(q)$. The propagator $g_2(q|q';t)$ which is the

conditional probability density of finding geminate pair $A^{-\bullet} + D^{+\bullet}$ at the instant of time t changes as a result of the relative diffusion motion of reactants of this pair [defined by a functional operator $\hat{L}_2(q)$], as well as due to geminate reactions of the pair $A^* + D$ generation (stage 7) and exciplex E_{gem} (stage 8). The term on the right-hand side of the second equation (3.15) describes the formation of the pair $A^{-\bullet} + D^{+\bullet}$ from the pair $A^{-\bullet} + S^{+\bullet}$ caused by bulk reaction of electron transfer from donor D to solvent molecule $S^{+\bullet}$ at the rate $k_1[D]$ (stage 3). The propagator $g_3(q|q';t)$ which is the conditional probability density of finding geminate pair $A^* + D$ at the instant of time t changes as a result of the relative diffusion motion of reactants of this pair [defined by a functional operator $\hat{L}_3(q)$], as well as due to geminate and bulk reactions of generation of exciplexes E_{gem} (stage 9) at the rate $w(q)$ and E_{bulk} at the rate $k_q[D]$, and monomolecular decay at the rate $\frac{1}{\tau_A}$ (stage 13). The term on the right-hand side of the third equation (3.15) describes the pair $A^* + D$ generation from geminate pair $A^{-\bullet} + D^{+\bullet}$ at the rate $w_2(q)$ (stage 7).

To calculate the sought quantum yields, we need only to know the steady-state quantities $p_N^s = p_N^L$ $(s = 0)$ $(N = A^*,$ $E_{bulk}, E_{gem})$, $g_i^s(q|q') = g_i^L(q|q'; s = 0)$ $(i = 1, 2, 3)$, and, accordingly, $I_N = I_N^L (s = 0)$ $(N = A, E)$. Note that all these quantities are positive, since p_N^s and $g_i^s(q|q')$ are the time integrals of the corresponding probabilities. Positivity of I_E follows from expression (3.14) for this source at $s = 0$, or, as positivity of I_A, from the first and the third steady-state equations for probabilities obtained from Eq. (3.13) at $s = 0$. Using definitions of steady-state sources and stationary equations derived from Eq. (3.14) for resolvents, we have the relation

$$I_A + I_E = 1 \quad \text{or} \quad I_A = 1 - I_E, \qquad (3.16)$$

so, due to positivity of the sources, $0 < I_A, I_E < 1$.

Solving algebraic equations (3.13) at $s = 0$ with allowance for Eq. (3.16), we obtain the ratio of luminescence quantum yields of exciplex and electron acceptor under X-ray irradiation

$$\mathrm{K}_{X-ray} = \frac{\tilde{\eta}_E}{\tilde{\eta}_A} = \frac{k_E^F}{k_A^F} \frac{p_E^L(s=0)}{p_A^L(s=0)} = \frac{k_E^F}{k_A^F} \tau_E k_q[D] (1 + C([D])),$$
$$(3.17)$$

where $C([D])$ is a quantity depending on concentration $[D]$ of electron donor D,

$$C([D]) = \frac{\left(k_q[D] + \frac{1}{\tau_A}\right) I_E}{(1 - I_E) k_q[D]} \quad (0 < I_E < 1). \qquad (3.18)$$

In the quantum yields ratio of Eq. (3.18), we replaced the steady-state rate constant k (3.4) of the bulk reaction of concentration excitation quenching (and exciplex accumulation) by the quenching rate constant (3.11) to take into account the transient (non-stationary) stage of this process. Note that, according to Eq. (3.11), the difference between the quenching constant and the steady-state rate constant results from the presence of intrinsic decay of the acceptor. Correspondingly, due to the absence of intrinsic decay, the bulk quenching rate constant of particle $A^{-\bullet}$(in geminate pair $A^{-\bullet} + D^{+\bullet}$) coincides with the steady-state constant k_1. Also note that the dependence on $[D]$ is more complicated than the dependence

explicitly appearing in Eq. (3.18), since the source I_E also depends on $[D]$.

Examination of the derived ratio of the quantum yields in the case of reaction initiation by X-irradiation K_{X-ray} (3.17) and the corresponding ratio for optical excitation initiation K_{Light} (3.12) shows that the first ratio demonstrates an increase in exciplex emission as compared to the second one, and this is exactly what is seen from the experiment. Of interest is also the quantity that shows that K_{X-ray} is greater than K_{Light},

$$\xi = \frac{\mathrm{K}_{X-ray}}{\mathrm{K}_{Light}} = 1 + C([D]) > 1. \qquad (3.19)$$

The non-negative quantity $C([D])$ is defined by the inhomogeneous terms (sources) in (3.14) (at $s = 0$) depending on the propagators of the corresponding reacting pairs that satisfy a set of equations (3.15) (at $s = 0$).

IV. DISCUSSION

The proposed multistage scheme (Scheme 2) of exciplex generation under X-irradiation makes it possible to describe the experimentally observed increase in the exciplex generation efficiency as compared to optical excitation (Fig. 5). The corresponding increase is defined by the quantity $C([D]) > 0$ in expression (3.19). The explicit form of its dependence on electron donor concentration $[D]$ can be calculated in the framework of specific model assumptions for reacting systems. However, expression (3.18), in view of equations for the source (3.14) and propagators (3.15), allows one to analyze the behavior of the function $C([D])$ at small concentrations of D.

Note that expression (3.18) is valid solely within a limited range of concentrations because of binary theory restrictions, so its analysis makes no sense at arbitrarily high concentrations. The range of concentration $[D]$ where the above theoretical description is valid is determined by the presence of a small parameter in the theory, namely, the density parameter ε,

$$\varepsilon = \frac{4}{3}\pi R_{eff}^3 [D] \ll 1, \qquad (4.1)$$

where R_{eff} is the "effective" radius of the reaction of two reactants. For the compounds under study (assuming contact interaction of reactants $R = 10^{-7}$ cm) at $\varepsilon = 0.1$ estimation shows that inequality (4.1) holds at concentrations $[D] \leq 0.04$ M. Any further increase in concentration leads to the necessity of taking into account triple encounters of reactants in solution, and, generally speaking, the behavior of the reacting system can substantially differ from the binary theory predictions. Thus we shall perform the subsequent analysis of experimental data in the concentration range $[D] \leq 0.04$ M restricting ourselves to the first four points of the dependence of ξ on DMA concentration in the mixture given in Fig. 5.

The source $I_E^L(s)$ describes the geminate channel of exciplex generation which is controlled, according to Scheme 2, by the formation of geminate pair $A^{-\bullet} + D^{+\bullet}$ from the pair $A^{-\bullet} + S^{+\bullet}$ due to the bulk reaction of electron transfer from donor D to solvent radical cation $S^{+\bullet}$ at the rate $k_1[D]$ (stage 3). So, as the donor concentration $[D]$ decreases, the exciplex generation efficiency through stage 3 also decreases, and
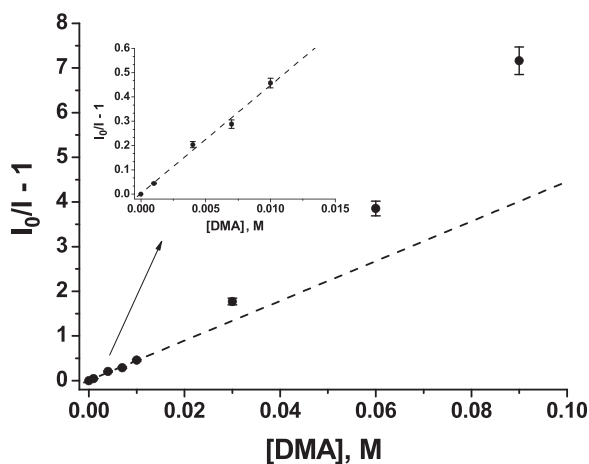
FIG. 6. Stern-Volmer plot for quenching of anthracene emission with DMA. Dashed line represents the least squares approximation of the first five points by a linear function: $I_0/I - 1 = 3 \cdot 10^{-3} + 44 \cdot [DMA]$. The range of low DMA concentrations is shown in the subplot. Error bars are 95% confidence intervals for each experimental point.

the source itself should tend to zero, with the actual limiting behavior depending on the details of the assumed model. To bridge the source behavior with experiment, an approximation over the first four points of the experimental dependence $K_{X\text{-ray}}/K_{Light}$ (Fig. 5) by expressions (3.18) and (3.19) was performed assuming a general power-law dependence of the source $I_E([D])$ on donor concentration $[D]$,

$$I_E([D]) \underset{[D] \to 0}{\sim} \alpha [D]^{\beta}. \qquad (4.2)$$

The required parameter $\tau_A k_q = 44 \pm 3$ M^{-1} appearing in Eq. (3.18) was obtained from the slope of experimental dependence $I_0/I - 1$ on the quencher concentration $[D]$, where I_0 is the anthracene luminescence intensity in the absence of DMA and I is the anthracene luminescence intensity with DMA present in the mixture. For this evaluation, luminescence spectra obtained in conditions of optical excitation with DMA concentration in the mixture up to 0.1 M [see Fig. 1(a)] were used. The obtained Stern-Volmer plot is shown in Fig. 6. The slope of the Stern-Volmer plot coincides with the

product of the lifetime τ_A available in the literature ($\tau_F = 5.6$ ns in *n*-hexane[22]) and the quenching rate constant k_q close to the diffusion-limited rate constant in isooctane ($1.3 \cdot 10^{10}$ M^{-1} s^{-1}[43]). The upper limit of the applicability of the binary theory ($[D] \leq 0.04$ M) referred to above is in a reasonable correspondence with the linear region of the obtained Stern-Volmer plot ($[D] \leq 0.02$ M).

Quite surprisingly, it was found that the best agreement with experiment took place at numerical values $\alpha \approx 0.19$, $\beta \approx 0$, if $[D]$ was measured in M. The derived parameter β means that the source I_E at small concentrations $[D]$ is a finite constant and does not tend to zero, as might be expected from considerations given above. Such a behavior unequivocally indicates a partial formation of geminate pairs $A^{-\bullet} + D^{+\bullet}$ with some initial distribution immediately after X-irradiation of solution, in addition to and not only due to bulk generation reaction 3 from the pair $A^{-\bullet} + S^{+\bullet}$. This fact may be accounted for by the instantaneous ionization mechanism discussed earlier, for example, in the interpretation of experimental data on the effective radius of electron transfer in non-polar solutions obtained by quantum beats.[44] The presence of initial distribution in the pair $A^{-\bullet} + D^{+\bullet}$ may be taken into consideration in Eq. (3.15) by applying appropriate initial conditions for the propagator g_2.

Substituting the obtained best fit approximation parameters, the numerical ξ dependence on $[D]$ takes the form

$$\xi = \frac{K_{X\text{-ray}}}{K_{Light}} \underset{[D] \to 0}{\sim} 1.23 + \frac{0.054}{[D]}. \qquad (4.3)$$

Its graph and comparison with experimental data are shown in Fig. 7.

For comparison, the best attainable approximation by a square root dependence on $[D]$ [$\alpha = 3.7$; $\beta = 0.5$ in Eq. (4.2)] is also shown.

More thorough investigation of experimental dependences calls for a detailed specification of all parameters of the reacting system. Deviations from the theoretical calculations are associated with simplification of the reaction scheme and incomplete account of all possible stages of exciplex generation under X-irradiation. For example, for the system under study at conditions of X-irradiation, along with the dominant
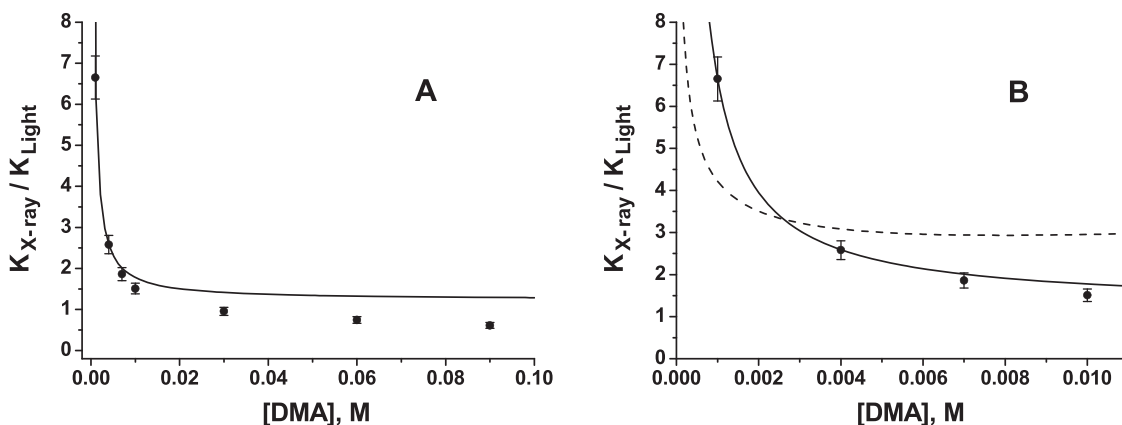

FIG. 7. (a) Dependence of the ratio $K_{X\text{-ray}}/K_{Light}$ on DMA concentration. Points—experimental data (see Fig. 5). Solid line—expression (4.3) over the entire concentration range. (b) Initial section of experimental concentration dependence of the ratio $K_{X\text{-ray}}/K_{Light}$, (four points), its approximation by expression (4.3) (solid line), and the best square root dependence ($\alpha = 3.7$; $\beta = 0.5$, dashed line). Error bars are 95% confidence intervals calculated by the error propagation law.

luminescence of electron acceptors (anthracene), there is some contribution of the electron donor (DMA) luminescence. As anthracene absorption spectra and DMA luminescence spectra substantially overlap, this can result in additional energy transfer to anthracene, which, in turn, will lead to an apparent decrease of the analyzed ratio $\xi = \frac{K_{\text{X-ray}}}{K_{\text{Light}}}$. The reason is that the channel of excited anthracene formation via energy transfer from DMA is possible under X-irradiation only; this leads to a decrease in $K_{\text{X-ray}}$, thus ξ. As a result, at high DMA concentration in the mixture, the parameter ξ may become less than 1, and this is easily seen from experimental data in Fig. 5 at DMA concentration above 0.03 M.

Further reaction channels that have so far been omitted from the analyzed reaction scheme include exciplex formation from excited DMA molecules, exciplex quenching by bulk collision with a DMA molecule, and triplet-triplet annihilation processes. Although a comprehensive scheme should probably include them all, estimates show that they are of only secondary importance for the purposes of this work. Regarding exciplex formation from D^* possible under X-irradiation, if we assume diffusion limited quenching with a rate constant of 10^{10} M^{-1} s^{-1}, we observe that with $2 \cdot 10^{-4}$ M of a quencher (in this case, anthracene) the quenching efficiency (the competition between exciplex formation $k_d[Q]$ and luminescence $1/\tau_F$) is very low, about 0.5%. This issue has been quantitatively explored in an earlier paper for the naphthalene-DMA system.[12] Exciplex quenching by DMA is certainly possible at high [DMA], as exciplex lifetime in this system is about 70 ns.[21] However, this process is equally possible under both optical excitation and X-irradiation, and its contribution to the suggested "ratio of ratios" metric $\xi = \frac{K_{\text{X-ray}}}{K_{\text{Light}}}$ is not expected to be large. This question certainly deserved further study. The possibility of triplet-triplet annihilation processes in a similar system has also been discussed in an earlier paper,[12] with the conclusion that at the used dose rate of X-irradiation they can be safely neglected unless very fine details need to be analyzed. Finally, in this work, a special non-luminescing alkane solvent has been used to simplify the reaction scheme, and generalization to an arbitrary alkane will require the introduction of additional channels involving the solvent excited state. We should also note that many of the additional channels that can be included in the reaction scheme will become important only at relatively high concentrations of DMA, and this requires abandoning the binary approximation of the theory which is a major theoretical challenge in itself. Such a closer examination and consistent derivation will be the subject of further publications.

V. SUMMARY

The article presents an experimental investigation of exciplex generation under optical and X-ray excitation using one and the same reacting system of non-polar solutions of anthracene and *N,N*-dimethylaniline. It was found that the ratio K_{Light} of the quantum yields of exciplexes and excited electron acceptors in the case of optical exciplex generation was less than the corresponding ratio $K_{\text{X-ray}}$ under X-irradiation. The dependence of the ratio $\xi = \frac{K_{\text{X-ray}}}{K_{\text{Light}}}$ on the concentration [D] of

the electron donor (DMA) in the mixture was experimentally obtained.

To interpret the obtained experimental results, theoretical schemes of reactions were proposed for which the corresponding quantum yields were calculated. Calculations were made on the basis of kinetic equations for the proposed multistage schemes of the bulk reaction of exciplex generation under optical excitation and bulk-geminate reaction of radical ion pairs under X-irradiation. These calculations explain the experimentally observed change in the ratio of the quantum yields of the excited electron acceptor and exciplex and the corresponding change in exciplex generation efficiency under X-irradiation as compared to the case of optical excitation. The analysis of the ratio ξ shows that its dependence on concentration [D] agrees with the main experimental results. To describe the concentration dependence in more detail, one should take into account additional channels of exciplex generation and consider a more complicated multistage reaction scheme.

SUPPLEMENTARY MATERIAL

See supplementary material for the details of decomposition experimental spectra obtained in different representations: wavelengths, wavenumbers, and transition dipole moment representation.

ACKNOWLEDGMENTS

[1] A. Mozumder, *Charged Particle Tracks and Their Structure: In Advances in Radiation Chemistry*, edited by M. Burton and J. L. Magee (Wiley, Interscience, New York, 1969), pp. 1–102.

[2] I. A. Shkrob, M. C. Sauer, Jr., and A. D. Trifunac, in *Radiation Chemistry of Organic Liquids: Saturated Hydrocarbons*, Studies in Physical and Theoretical Chemistry Volume 87, edited by C. D. Jonah and B. S. Madhava Rao (Elsevier, The Netherlands, 2001), Chap. 9, pp. 175–221.

[3] H. Leonhardt and A. Weller, Ber. Bunsenges. Phys. Chem. **67**, 791 (1963).

[4] N. Mataga and H. Miyasaka, "Electron transfer and exciplex chemistry," in *Electron Transfer: From Isolated Molecules to Biomolecules*, Advances in Chemical Physics, Part 2, edited by J. Jortner and M. Bixon (Wiley, New York, 1999), Vol. 107, pp. 431–496.

[5] S. A. Jenekhe and J. A. Osaheni, Science **265**, 765 (1994).

[6] J. F. Wang, Y. Kawabe, S. E. Shaheen, M. M. Morrell, G. E. Jabbour, P. A. Lee, J. Anderson, N. R. Armstrong, B. Kippelen, E. A. Mash, and N. Peyghambarian, Adv. Mater. **10**, 230 (1998).

[7] M. Okazaki, Y. Tai, R. Nakagaki, K. Nunome, and K. Toriyama, Chem. Phys. Lett. **166**, 227 (1990).

[8] E. J. Land, J. T. Richards, and J. K. Thomas, J. Phys. Chem. **76**, 3805 (1972).

[9] C. P. Keszthelyi and A. J. Bard, Chem. Phys. Lett. **24**, 300 (1974).

[10] J. B. Ketter and R. M. Wightman, J. Am. Chem. Soc. **126**, 10183 (2004).

[11] A. R. Melnikov, E. V. Kalneus, V. V. Korolev, I. G. Dranov, and D. V. Stass, Dokl. Phys. Chem. **452**, 257 (2013).

[12] A. R. Melnikov, E. V. Kalneus, V. V. Korolev, I. G. Dranov, A. I. Kruppa, and D. V. Stass, Photochem. Photobiol. Sci. **13**, 1169 (2014).

[13] V. M. Agranovich and M. D. Galanin, *Electron Excitation Energy Transfer in Condensed Matter* (North-Holland, Amsterdam, 1982).

[14] E. V. Kalneus, A. R. Melnikov, V. V. Korolev, V. I. Ivannikov, and D. V. Stass, Appl. Magn. Reson. **44**, 81 (2013).

[15] I. B. Berlman, *Handbook of Fluorescence Spectra of Aromatic Molecules* (Academic Press, New York, 1971).

[16] W. Rothman, F. Hirayama, and S. Lipsky, J. Phys. Chem. **58**, 1300 (1973).

[17] R. Hermann, R. Mehnert, and L. Wojnárovits, J. Lumin. **33**, 69 (1985).

[18] A. R. Melnikov, V. N. Verkhovlyuk, E. V. Kalneus, V. V. Korolev, V. I. Borovkov, P. S. Sherin, M. P. Davydova, S. F. Vasilevsky, and D. V. Stass, Z. Phys. Chem. **231**, 239 (2017).

[19] J. R. Lakowicz, *Principles of Fluorescence Spectroscopy*, 3rd ed. (Springer, New York, 2006).

[20] G. Angulo, G. Grampp, and A. Rosspeintner, Spectrochim. Acta, Part A **65**, 727 (2006).

[21] A. R. Melnikov, E. V. Kalneus, V. V. Korolev, P. S. Sherin, V. I. Borovkov, and D. V. Stass, Photochem. Photobiol. Sci. **15**, 767 (2016).

[22] E. Blatt, F. E. Treloar, K. P. Ghiggino, and R. G. Gilbert, J. Phys. Chem. **85**, 2810 (1981).

[23] O. A. Anisimov, *Ion Pairs in Liquids: In Radical Ionic Systems: Properties in Condensed Phases*, edited by A. Lund and M. Shiotani (Springer, The Netherlands, 1991), pp. 285–309.

[24] A. Weller, Z. Phys. Chem. **130**, 129 (1982).

[25] A. Weller, H. Staerk, and R. Treichel, Faradey Discuss. Chem. Soc. **78**, 271 (1984).

[26] S. G. Fedorenko and A. I. Bursthein, J. Phys. Chem. A **114**, 4558 (2010).

[27] S. G. Fedorenko, S. S. Khokhlova, and A. I. Burshtein, J. Phys. Chem. A **116**, 3 (2011).

[28] S. G. Fedorenko and A. I. Burshtein, J. Chem. Phys. **141**, 114504 (2014).

[29] J. B. Birks and I. H. Munro, "The fluorescence lifetimes of aromatic molecules," in *Progress in Reaction Kinetics* Volume 4, edited by Porter G. (Pergamon Press, Oxford, 1969), pp. 239–303.

[30] T. R. Waite, J. Chem. Phys. **28**, 103 (1958).

[31] M. von Smoluchowski, Z. Phys. Chem. **92**, 129 (1917).

[32] F. C. Collins and G. E. Kimball, J. Colloid Interface Sci. **4**, 425 (1949).

[33] A. B. Doktorov, *Development of the Kinetic Theory of Physicochemical Processes Induced by Binary Encounter of Reactants in Solutions: In Recent Research Development in Chemical Physics*, edited by S. G. Pandalai (Transworld Research Network, Kerala, India, 2012), Vol. 6, Chap. 6, pp. 135–192.

[34] M. Yokota and O. Tonimoto, J. Phys. Soc. Jpn **22**, 779 (1967).

[35] I. Z. Steinberg and E. Katchalski, J. Chem. Phys. **48**, 2404 (1968).

[36] K. L. Ivanov, N. N. Lukzen, and A. B. Doktorov, J. Chem. Phys. **145**, 064104 (2016).

[37] A. A. Kipriyanov, O. A. Igoshin, and A. B. Doktorov, Physica A **268**, 567 (1999).

[38] A. I. Burshtein, I. V. Gopich, and P. A. Frantsuzov, Chem. Phys. Lett. **289**, 60 (1998).

[39] A. B. Doktorov, J. Chem. Phys. **141**, 104104 (2014).

[40] L. Monchick, J. Chem. Phys. **24**, 381 (1956).

[41] S. G. Fedorenko, A. A. Kipriyanov, and A. B. Doktorov, Phys. Res. Int. **2011**, 451670.

[42] A. B. Doktorov and A. A. Kipriyanov, J. Chem. Phys. **140**, 184104 (2014).

[43] M. Montalti, A. Credi, L. Prodi, and M. Teresa Gandolfi, *Handbook of Photochemistry*, 3rd ed. (CRC Press, Taylor & Fransis Group, Boca Raton, Fl, USA, 2006).

[44] T. V. Kobzeva, V. A. Bagryanskii, and Y. N. Molin, Dokl. Phys. Chem. **387**, 304 (2002).